Quantum Molecular Dynamics

Simulating Warm, Dense Matter

Lee A. Collins, Joel D. Kress, and Stephane F. Mazevet

Regions of warm, dense matter abound—from the interiors of giant gaseous planets, such as Saturn, and the atmospheres of white dwarf stars to laboratory plasmas in high-energy density generators and inertial confinement fusion capsules. Warm, dense matter, a sizzling "soup" of atoms, molecules, ions, and free electrons, is difficult to describe by standard techniques because it harbors multiple species and processes simultaneously—from ionization and recombination to molecular dissociation and association. Recently, quantum molecular dynamics (QMD), which can predict static, dynamical, and optical properties from a single, first principles framework, has been used to accurately predict properties of hydrogen, oxygen-nitrogen mixtures, and plutonium in the warm, dense state.

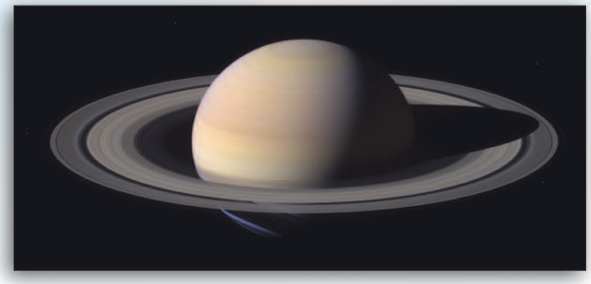

At the core of Saturn, there is warm, dense matter, ranging between 5000 and 6000 kelvins in temperature.

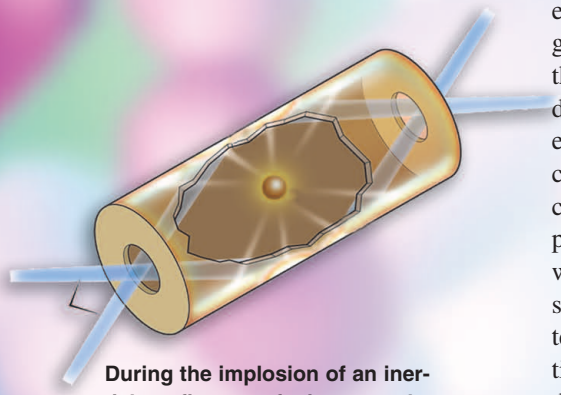

During the implosion of an inertial confinement fusion capsule, the deuterium-tritium atoms it contains become warm, dense matter.

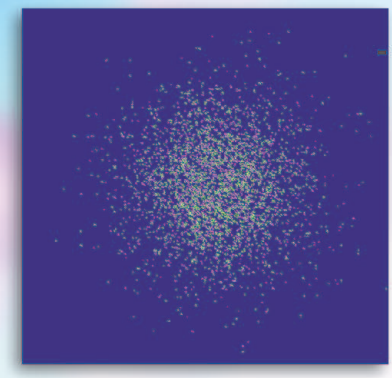

This ultracold neutral plasma of electrons (green dots) and protons (pink dots) was created by heating microkelvin matter with a laser pulse. Surprisingly, this strongly coupled plasma has many features in common with warm, dense matter.

Warm, dense matter (WDM) appears in a wide variety of celestial and terrestrial environments—from the interiors of gaseous planets and atmospheres to the plasmas generated by high-energy-density machines and lasers. Other examples include shock-compressed cryogenically cooled materials, ultracold plasmas, and various stages in primary and secondary nuclear weapons. In general, these systems span temperatures from hundreds to tens of millions of kelvins and densities from about 1/100 to 100 times the density of a solid. The medium in each system resembles a "soup" of various species—including atoms, molecules, ions, and electrons—that exhibits distinctly nonclassical behavior in the interaction of all the particles. This material state is now generally referred to as warm, dense matter.

To model such systems, we have applied quantum molecular dynamics (QMD) simulation methods that treat the rapidly moving electrons quantum mechanically and the sluggish nuclei classically. In order to provide a diverse and systematic representation of the quantum mechanical effects, we have treated the electrons at various levels of sophistication—from a simple semi-empirical tight-binding model to a state-of-the-art finite-temperature density functional theory (DFT) approach. Because these techniques begin with only the most basic assumptions on the nature of the microscopic particle interactions from which all the macroscopic properties derive, they are designated as ab initio, or "from first principles." Through the QMD prescription, we can represent very complex structural and dynamical quantum processes that dominate these media. These methods currently allow for the treatment of a few hundred particles; however, scaling tests for massively parallel computers indicate that simulations with thousands of atoms will shortly become routine. An additional advantage of the QMD methods comes from their integrated nature. Because the QMD framework describes the elemental particle interactions, all the static, dynamical, and optical properties can be derived from an internally consistent set of principles, whereas in many models of dense media, the representations of these processes arise from different approaches at different levels of approximation.

The representation of a warm, dense system as an evolving sample of particles interacting through quantum mechanical forces has become possible only within the last two decades with the development of supercomputing capabilities. Los Alamos has pioneered this endeavor. As early as 1985, prototypical models, based on a semi-empirical determination of the quantum forces in representative snapshots of atomic configurations derived from classical molecular dynamics (MD) simulations, indicated the potential of such integrated approaches. By the mid 1990s, density functional methods had matured to the extent of effectively treating atomic samples of about 100 particles, a threshold for obtaining statistically significant macroscopic properties. This development initiated a renewed effort to employ these techniques together with semi-empirical approaches to model warm, dense systems. The ensuing years have witnessed the steady improvement of the basic quantum mechanical methods, efficient algorithms, and computational power, providing great accuracy in the characterization of these media.

Quantum Molecular Dynamics

A three-dimensional reference cell, containing N atoms (nuclei) at positions $\mathbf{R}[= \{\mathbf{R}_1 \ldots \mathbf{R}_N\}]$ and instanta-

neous momenta $\mathbf{P}[= \{\mathbf{P}_1 \ldots \mathbf{P}_N\}]$ and N_e electrons at $\mathbf{r}[= \{\mathbf{r}_1 \ldots \mathbf{r}_{Ne}\}]$, determines the basic working unit in QMD calculations. In order to represent the extended nature of the medium, we periodically replicate this cell throughout space and treat particle interactions both within the reference cell and with the repeated cells. The system evolves temporally according to a repeated two-step prescription. First, for fixed nuclear positions $\mathbf{R}(t)$ at a time t, we perform a sophisticated quantum mechanical calculation for the electrons. From the resulting electronic wave function $\Psi[\mathbf{r},\mathbf{R}]$, which depends only parametrically on the nuclear positions $\mathbf{R}$, we determine a force on each atom. Second, using this quantal force, we advance the nuclei over a short time δt by the classical equations of motion, yielding a new set of positions $\mathbf{R}(t + \delta t)$ and momenta $\mathbf{P}(t + \delta t)$ for the nuclei. This two-step process for temporally evolving a collection of particles forms the core of most MD approaches; the "Q" in QMD arises from the use of quantum mechanics to describe the electronic component.

We calculate the electronic many-body wave function $\Psi[\mathbf{r},\mathbf{R}]$ by solving the Schrödinger equation:

$$H\,\Psi[\mathbf{r},\mathbf{R}] = E\,\Psi[\mathbf{r},\mathbf{R}] \quad ,$$

where the Hamiltonian operator H has the form

$$H = T_e + V_{ee} + V_{eN} + V_{NN} \quad .$$

T_e represents the kinetic energy of the electrons (e), and V_{ab} gives the interaction between the electrons (ee), the electrons and the nuclei (eN), and the nuclei (NN).

Numerous methods exist for solving the Schrödinger equation; however, the two most popular either construct the multicoordinate state function Ψ directly or employ the electron density $n(\mathbf{r}_i)$, determined by integrating the probability density $|\Psi|^2$ over all but one spatial variable. This density depends on only a single point in space and forms the basis of density functional theory (DFT). Both approaches usually invoke decomposition into single-electron orbitals, which in turn are expanded in a basis of simple functions such as Gaussians or plane waves. This reduction transforms the Schrödinger equation into a matrix eigenvalue problem for which powerful iterative techniques can effectively produce solutions.

We employ the wave function approach to generate an efficient, approximate procedure for solving the Schrödinger equation and rapidly advancing the molecule dynamics equations. In this tight-binding technique, we replace the matrix elements of H with semi-empirical forms fit to experimental data and specific theoretical results. The method still contains all the important processes afoot in the WDM regime: molecular dissociation and association, ionization and recombination, as well as electron collision and attachment.

In DFT, we use a very accurate form of these matrix elements that includes all the basic electrostatic and quantum effects (exchange and correlation). Although more expensive to calculate, this formulation yields a very accurate representation of a many-electron system. We typically use an extended form of DFT that includes finite temperature effects and some nonlocality (generalized gradient approximation). Most simulations evolve in local thermodynamical equilibrium with the electronic and nuclear kinetic temperatures set equal.

As indicated, for each MD time step, we obtain a set of positions and momenta $\{\mathbf{R}(t),\mathbf{P}(t)\}$ for the nuclei and the quantum mechanical state function $\Psi[\mathbf{r},\mathbf{R}]$ for the electrons. From this information, we can determine static properties, such as pressure and internal energies, and thus the equation of state (EOS), as well as dynamical properties such as diffusion, viscosity, order parameters, and thermal conductivities. On the other hand, the state function for the electrons yields optical properties such as electrical conductivity, reflectivity, dielectric functions, and opacities. The derivation of these properties from an internally consistent set of basic quantities $[\mathbf{R},\mathbf{P},\Psi]$ highlights a critical advantage of the QMD formulation.

The large variety of systems and environments explored by the QMD approaches attests to their great flexibility and applicability. Such applications include the following: isotopic plasma mixtures of dense hydrogen, nitrogen, and oxygen; highly compressed rare-gas solids, alkali metals near melt and along the vapor-liquid coexistence boundary, impurity atoms in dense hydrogen plasmas, shock-compressed liquids of atoms and hydrocarbons, and disorder in semiconductors.

For some of these cases, detailed experimental data exist. The generally good agreement obtained with the results of QMD simulations provides an effective validation of the technique across an extensive range of conditions and media. This validation proves particularly critical for the deployment of QMD into regimes of matter under extreme conditions, totally inaccessible to current experiments but vitally important to many national missions.

As a demonstration of the efficacy of these methods, we consider several representative examples.

Static Properties: Equation of State

The EOS of a material gives pressure and internal energy as a function of density and temperature and forms a basic component of any

model of a macroscopic system. The shock Hugoniot experiment provides the principal means of probing equations of state. In this case, a well-characterized shock is driven through a medium by the impact of a flier plate (from either a gas gun or a high-energy density device) or of a high-intensity laser pulse. The shock pressures (P), densities (ρ), and specific internal energies are determined by the Rankine-Hugoniot jump conditions across the thin shock front. These equations relate flow velocities and thermodynamical variables in the shocked state to those in the initial state. Therefore, knowing the initial conditions and the EOS, we can determine the value of the pressure—for example, at the final conditions—and compare with experimental observations.

As a first example, we focus on hydrogen, both for its deceptive simplicity and for the considerable controversy that has raged over its EOS. From an atomic physics standpoint, hydrogen, having but one proton and one electron, is the simplest element known. Surprisingly, its phase diagram displays considerable complexity. For a temperature range between 10^4 and 10^5 kelvins and a density range between 0.1 and 1.0 gram per cubic centimeter (g/cm^3), hydrogen exists as a dense diatomic fluid. As the temperature and density increase, the fluid undergoes continuous dissociation and ionization to become a fully ionized plasma consisting solely of free electrons and protons. For this regime, the challenge in obtaining a meaningful EOS lies in accurately describing the evolution of the delicate balance of atomic, molecular, and ionized species constituting the fluid. This complicated nature of hydrogen becomes evident in Figure 1, which displays the electronic probability density around the nuclei for a snapshot within a QMD simulation.

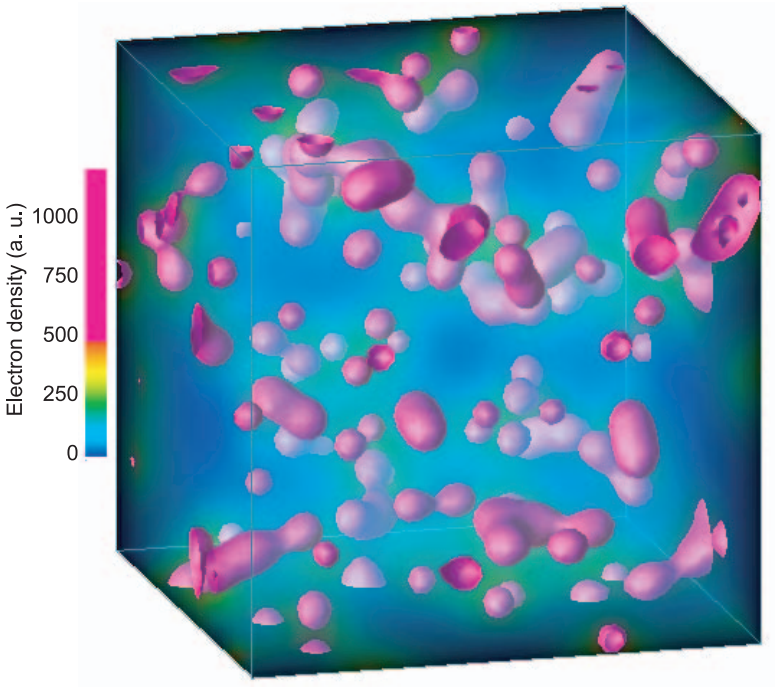

Figure 1. QMD Simulation of Hydrogen Electronic Density
A three-dimensional snapshot of a representative cubic sample of 128 highly compressed hydrogen atoms (1 g/cm^3 at 29,000 K) at a particular time within the QMD simulation shows the probability of finding an electron at a particular location. Magenta indicates the highest probability; blue, the lowest. The electron density indicates the presence of molecular systems (magenta ellipsoidal structures), atomic systems (magenta spheres), and free electrons in the intervening space.

The EOS of hydrogen and its isotope deuterium has received new attention because of recent laser experiments that seemed to call into question older models. Figure 2 displays the current status and depicts the pressure as a function of density for the shock compression (or the Hugoniot) of a molecular deuterium sample that was, at first, cryogenically cooled. Until the laser experiments, the established Hugoniot came from a chemical model in the SESAME equation of state tables compiled at Los Alamos in the 1970s, which yielded a maximum compression $\eta = 4$, given by the ratio of the density ρ to the initial density of the sample ρ_0. Experiments at the NOVA laser facility of the Lawrence Livermore National Laboratory (Lawrence Livermore) indicated a far more compressible medium with $\eta = 6$. This difference has profound ramifications for such diverse fields as planetary interiors (refer to Saumon and Guilot 2004) and nuclear weapons.

To gain insight into this experimental disagreement, we performed QMD calculations using the simple semi-empirical, tight-binding MD method and the very sophisticated density function approach (DFT-MD). Our QMD values agreed much better with the SESAME results and with subsequent, similar ab initio calculations—for example, the Path Integral Monte Carlo (PIMC). This agreement between the QMD and PIMC results has an

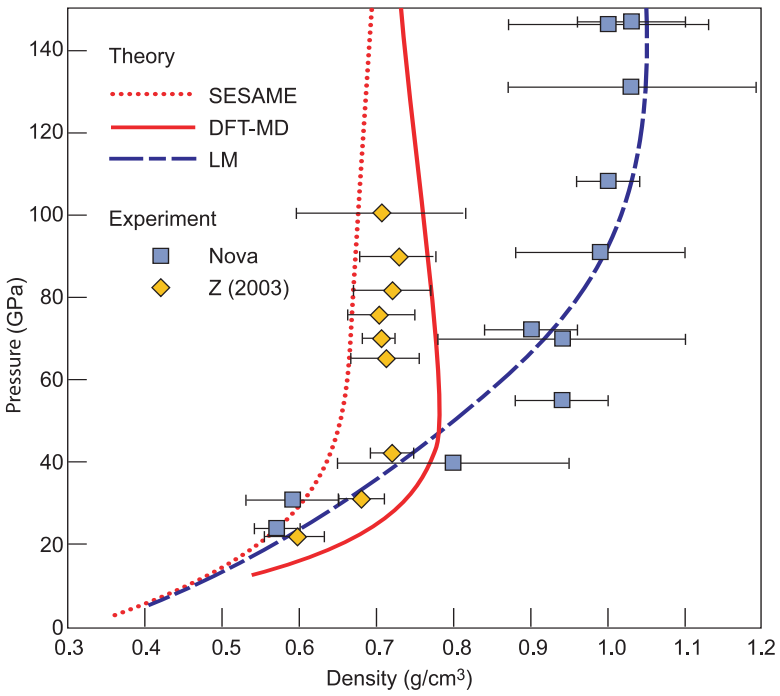

Figure 2. The Principal Hugoniot of Deuterium
The curves in this plot represent theoretical results from QMD simulations (DFT-MD) and from two free-energy minimization models, one used in the SESAME tables and the other based on linear mixing (LM). The experimental results are from the NOVA laser at Lawrence Livermore and the Z-machine at Sandia in New Mexico.

additional poignancy in that the PIMC treats the electronic and nuclear interactions by an approach completely independent of DFT. In 2000, a new set of experiments at the Sandia National Laboratories (Sandia), employing a flier plate accelerated by a pulse-power machine (Z-machine), produced results in close accord with the ab initio methods. Finally, within the last two years, Russian experiments (conducted at Sarov) with explosively generated converging shock waves supported the Sandia findings. The final verdict on the EOS of hydrogen awaits further experimental trials; however, the good agreement between the ab initio MD simulations and the experiments at the Z-machine and in Russia gives a strong penchant for the stiffer compressibility of hydrogen.

As a second example of the broad applicability of these approaches, we present comparisons of QMD simulations for compressed molecular nitrogen, oxygen, and nitrogen oxide (NO), which are similar to hydrogen in some respects: They all have molecular liquid states at very low temperatures, large dissociation energies, and moderate ionization potentials. For these three species though, several gas-gun experiments have probed a larger span of the Hugoniot than for hydrogen. Figure 3 displays the excellent agreement obtained between the QMD simulations and the experiments for the three species along the principal Hugoniot. This agreement indicates that the QMD approach can accurately characterize the progress of a very complex medium through many different stages. For example, the kink seen to varying degrees in all three Hugoniots indicates the transition from a molecular to an atomic fluid.

Experiments rarely follow the full evolution of a system but usually provide only final conditions based on prescribed starting values. On the other hand, QMD simulations can continuously monitor the state of the medium, yielding such valuable information as its constitution. To obtain better insight into the temporal development of a stressed medium, we examined, as a representative system, NO during compression from a cryogenic molecular liquid to a warm, dense fluid. The pair correlation function $g_{\alpha\beta}(r)$, which gives the probability of finding particles of type β a given distance r from a reference particle of type α, serves as an effective tool for tracing the change in the constituents. Figure 4(a) shows the conditions near the start of the compression in which the system consists mainly of NO molecules, as evidenced by the large peak in $g_{\mathrm{NO}}(r)$ at the average internuclear separation $R_{eq}(\mathrm{NO})$ for the molecular species. As both the density and temperature increase, the NO dissociates, and the freed nitrogen atoms combine into nitrogen molecules, but the oxygen remains in an atomic state. Figure 4(b) clearly depicts this behavior by the large peak in $g_{\mathrm{NN}}(r)$ near $R_{eq}(\mathrm{N_2})$ and the very weak peak around $R_{eq}(\mathrm{O_2})$. This finding challenges the present assumptions on modeling NO in overdriven shocks and has significant ramifications for explosives and high-pressure reactive chemistry.

Optical Properties

From the wave function that characterizes the electrons, we can also generate optical properties for the medium, including absorption coefficients, dielectric functions, reflectiv-

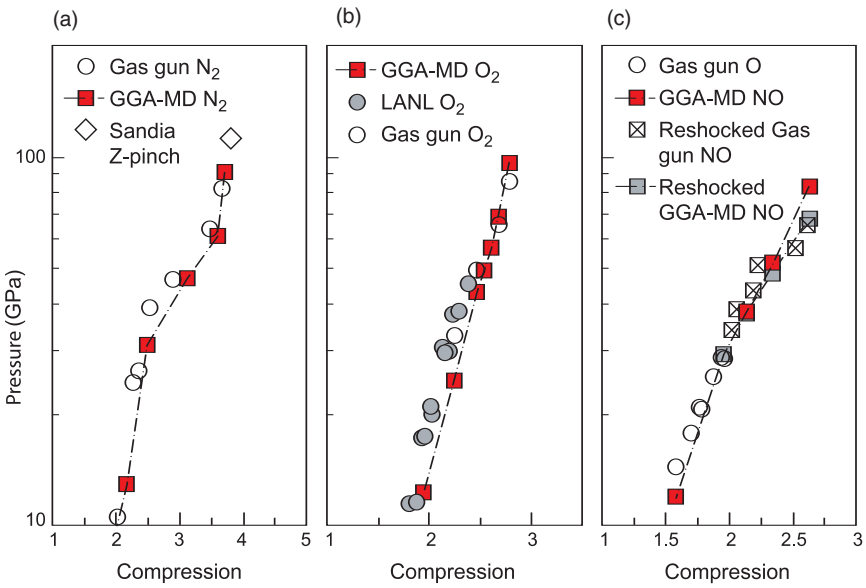

Figure 3. QMD vs Experiment for the Principal Hugoniot of N_2, O_2, and NO

Pressure is shown as a function of compression ($\eta = \rho/\rho_0$) along the principal Hugoniot for nitrogen (a), oxygen (b), and NO (c). Each panel compares QMD theoretical results (GGA-MD, red squares) with gas gun and Z-pinch experiments. In (c) reshock results are also shown. The excellent agreement between theory and experiment is noteworthy.

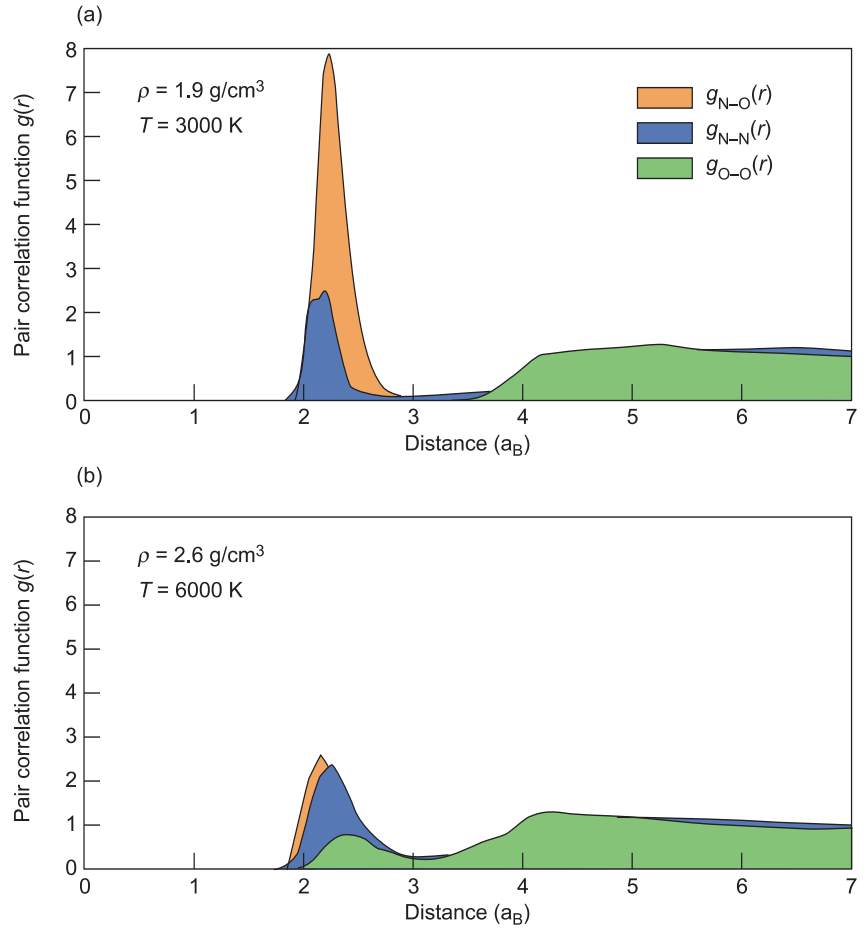

Figure 4. Pair Correlation Function for a NO Fluid under Shock Compression

The $g(r)$ pair correlation function gives the probability of finding an atom of a particular type a distance r from a reference atom. It therefore yields information about the composition of the fluid. The panels depict two sets of conditions: (a) density = 1.9 g/cm^3 and temperature = 3000 K, and (b) density = 2.6 g/cm^3 and temperature = 6000 K. The fluid begins as a pure system of NO molecules. As the temperature and density increase under compression, the NO dissociates and nitrogen molecules form. Oxygen remains almost entirely atomic.

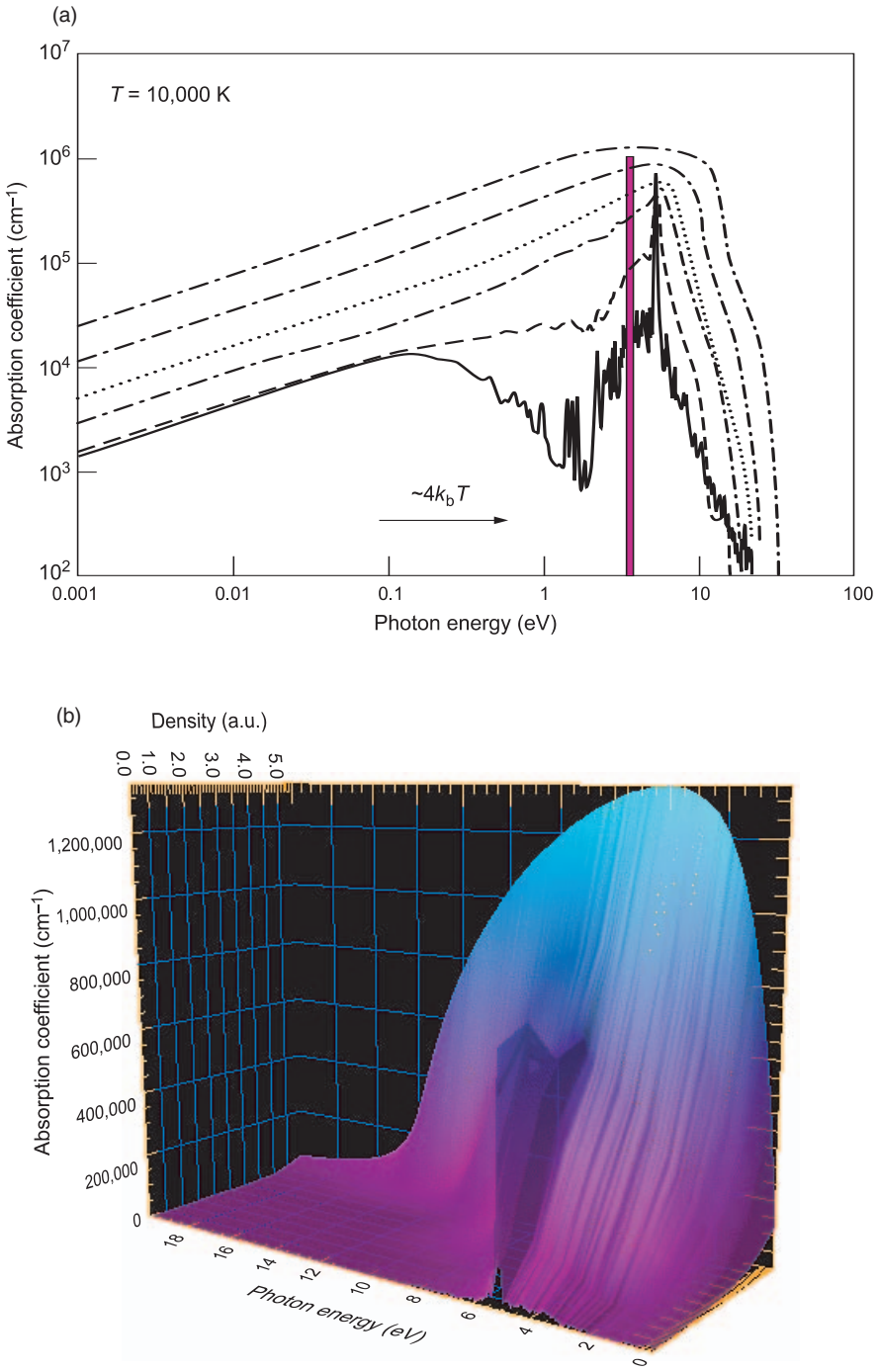

Figure 5. QMD Results for the Aluminum Absorption Coefficient
(a) From highest to lowest, the curves in this plot represent densities from 2.0 g/cm^3 to 0.025 g/cm^3 and show the trend in optical properties as the system moves from a solid to a gas. The absorption coefficient at the lowest density exhibits a distinct spectral line around 5 eV, originating from the 3s to 3p atomic transition. As the density increases, this feature broadens and melds with the continuous background. At the highest density, the profile resembles that of a dense metallic fluid. (b) The lower panel presents the same information but with a separate density axis.

ities, indices of refraction, and opacity. Opacity, a measure of the absorption of radiation in matter, is an important quantity in modeling diverse phenomena in astrophysics and in designing weapons. Many of the opacity libraries commonly used for standard macroscopic modeling programs (for example, in hydrodynamics) employ physical models that have not seen significant revision in decades. During this time, developments in a wide variety of fields, including weapons, inertial confinement fusion, high-energy density, and astrophysics, have required extensions of these libraries into new and complex regimes. Such an extension requires careful validation, either from experiments or from more-sophisticated theoretical methods, of the physical models that produce the opacity data. Since experiments have proved difficult within these new realms, as witnessed by the controversy over the EOS of compressed deuterium, ab initio simulation techniques, such as QMD, provide the best venue for making meaningful critiques of these models.

As indicated, these ab initio approaches produce a consistent set of material and optical properties from the same simulation. In contrast, the opacity libraries consist of a collection of approximate models. Therefore, an understanding of the differences in the opacities between the libraries and ab initio approaches requires a detailed examination of the underlying material properties, such as the EOS, and optical properties (absorption coefficient). To this end, we have performed large-scale QMD simulations of hydrogen and of aluminum and compared representative properties with the results from standard opacity libraries, in particular, the Light Element Detailed Configuration Opacity (LEDCOP) Code from Los Alamos.

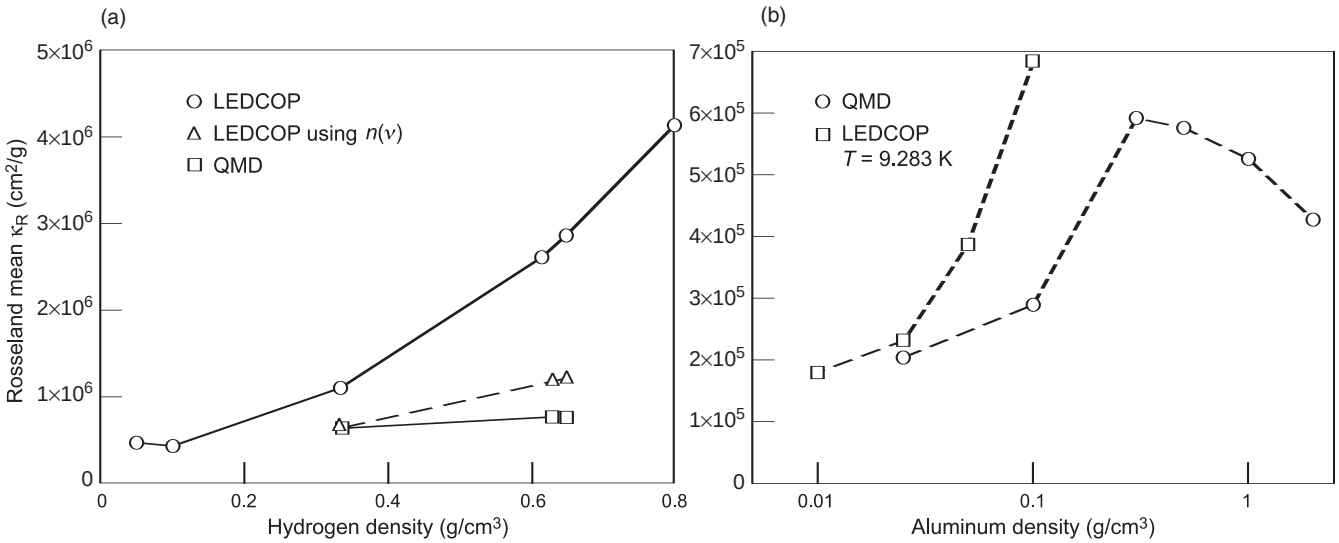

Figure 6. QMD- and LEDCOP-Derived Rosseland Mean Opacities for Hydrogen and Aluminum
We used QMD and LEDCOP to obtain Rosseland mean opacities as a function of density for hydrogen (a) and aluminum (b) at fixed temperatures of 48,000 K and 10,000 K, respectively. LEDCOP is based on an isolated atom perturbed by the surrounding medium; QMD considers all the atoms in the reference cell on an equal footing. "LEDCOP using $n(\nu)$" is based on the isolated atom absorption coefficient and the QMD index of refraction. At low densities in the gas phase, LEDCOP and QMD agree well. As the density increases, the effects of the medium become pronounced, and the perturbative treatment fails.

The absorption coefficient $\alpha(\nu)$, which gives the attenuation of radiation as a function of frequency ν (photon energy) at a given density ρ and temperature T, is the fundamental physical quantity determined by both the QMD and LEDCOP. This quantity has a direct relationship to the frequency-dependent electrical conductivity $\sigma(\nu)$ and index of refraction $n(\nu)$ of the medium [$\alpha(\nu) = 4\pi\sigma(\nu)/n(\nu)$]. For zero frequency, $\sigma(\nu)$ yields the more familiar direct-current (dc) electrical conductivity σ_{dc}[$= \sigma(0)$], which determines the degree of current flow in a substance. Materials with σ_{dc} above 10,000 per ohm centimeter (Ω cm) are considered good conductors or metals; those with σ_{dc} below 1000 $(\Omega\ \text{cm})^{-1}$, quasi-metals, or near insulators. Finally, the inverse of $\alpha(\nu)$, integrated in frequency over the derivative of the normalized Planck function, yields the ubiquitous Rosseland mean opacity κ_R.

Figures 5(a) and 5(b) portray, from different perspectives, the absorption coefficient as a function of photon energy at a given temperature (10,000 kelvins) for aluminum, as the metal passes between two very different physical states: from a warm fluid at solid density (2.0 g/cm^3) to a gas (0.025 g/cm^3). The finite value of $\alpha(\nu)$ at low frequencies implies a conducting medium of varying degrees. At high densities, the associated σ_{dc} of about 30,000 $(\Omega\ \text{cm})^{-1}$ indicates a metallic fluid, whereas the small values—<1000 $(\Omega\ \text{cm})^{-1}$—in the gas phase signify an almost insulating medium. For the gas, we also note the appearance of structure in the absorption coefficient. The peak around 5 electron volts corresponds to the atomic line of neutral aluminum for the transition from 3s to 3p. This transition again identifies the low-density state as a collection of neutral atoms with a few free electrons. The bar at an energy corresponding to $4k_BT$ represents the regime with maximum contribution to the mean opacity.

In Figure 6, we compare QMD and LEDCOP calculations of the Rosseland mean opacity κ_R at a fixed temperature as a function of density for both hydrogen and aluminum. As the density decreases, the two approaches show better agreement. This agreement follows from the nature of the LEDCOP model, in which density effects enter only perturbatively upon an isolated atom. For higher densities, the strong overlap among the wave functions on different atomic centers obviates this perturbative view and needs a more democratic treatment of all the system electrons. This comparison demonstrates the ability of QMD simulations to validate and improve current opacity libraries as they are extended into new regimes.

Dynamical Properties

Plutonium may very well be the most complex of elements. At atmospheric pressure, the phase diagram shows six equilibrium solid phases as well as a liquid phase. A study of plutonium introduces another level of complexity because

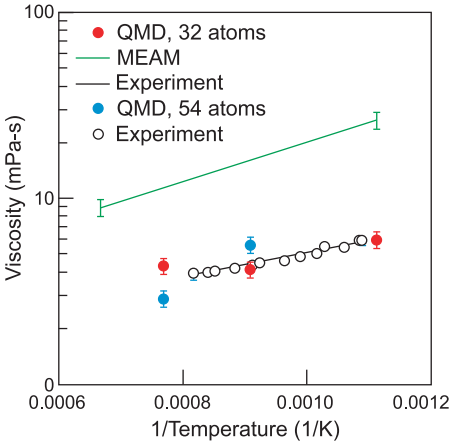

Figure 7. Temperature Dependence of Plutonium Viscosity

Molecular dynamics simulations are compared with a quantum mechanical (QMD) approach (red and blue squares) and a classical-potential (MEAM) approach (green line). QMD results are for samples of 32 atoms (red squares) and 54 atoms (blue squares). Experimental points are indicated by open squares. Quantum-derived forces appear important in determining the dynamic properties of this heavy system.

electron spin (magnetic behavior) must also be considered. Although the spin-DFT calculations for the face-centered-cubic (fcc) lattice structure (δ-plutonium) predict an antiferromagnetic (AF) state (in disagreement with the observations of a nonmagnetic state), the predicted structure is quite good, with an atomic volume (V) about 9 percent less than experiment. (An AF state has a net zero magnetic moment, with spin directions alternating up and down at each atomic site on the lattice.) We proceeded to study liquid plutonium with QMD in order to explore whether the quantum-derived forces provide a better description than does the interatomic potential of the classical Modified Embedded Atom Method (MEAM). We worked under the hypothesis that the predicted spin-DFT structural behavior will dominate over the predicted magnetic behavior, especially because the latter should be diminished by the disorder introduced in the liquid structure. An AF-like solution was found for the spin-DFT calculation (net zero magnetic moment with spins allowed to fluctuate on each atom during the MD trajectory). Radial distribution functions were calculated and self-diffusion coefficients (D) were derived from the mean-squared displacement of the atoms determined from the MD trajectory. In Figure 7, we compare QMD and classical MD (employing the MEAM potential) calculations of the viscosity of liquid plutonium with experimental data. In the classical MD calculations (performed by Los Alamos scientists Frank Cherne of the Materials Dynamics Group, Michael Baskes of the Structure/Property Relations Group, and Brad Holian of the Theoretical Chemistry and Molecular Physics Group), a 1024-atom simulation cell and nonequilibrium driven-slab boundary conditions were employed to compute the viscosity directly. In the QMD simulations, we calculated D from the mean-squared displacement of the atoms determined from an equilibrium MD trajectory and a 54-atom cell. The viscosity (η) was then calculated from a Stokes-Einstein relationship, namely, $(D\eta b)/(k_b T) = c$, where $b = V^{1/3}$ and k_b = Boltzmann constant. The dimensionless constant $c = 0.18$ ($\pm$ 0.02) is based on an analysis of experimental data for 21 different liquid metals (this work was conducted by Eric Chisolm and Duane Wallace of the Mechanics of Materials and Equation-of-State Group at Los Alamos). (A value of $c = 0.154 \pm 0.0123$ was determined from the classical MD simulations.) The MEAM potential was developed to describe the solid phases of plutonium; therefore, the results from the liquid simulations are a prediction. In this light, the MEAM values in Figure 7 are in fair agreement with experiment (within a factor of 5). The preliminary QMD results agree reasonably well with experiment, although we note that a 54-atom simulation is probably too small to provide a definitive answer.

Preliminary simulations at 1300 kelvins for (a) 54 atoms with the net zero magnetic moment relaxed and for (b) 108 atoms (requiring at least 32 Pentium processors in parallel) are yielding viscosities consistent with those illustrated in Figure 7. The relaxed magnetic moment result illustrates that the magnetic state apparently has little influence on the structure and dynamics of the liquid. With more computational horsepower, our goal is to calculate viscosity directly with QMD using nonequilibrium MD boundary conditions and 1024 atoms.

In summary, QMD simulations have proved an effective, versatile theoretical and computational approach to treating a large variety of warm, dense systems of particular interest to a broad number of Laboratory programs by providing systematic, integrated techniques for probing matter under extreme conditions. ■

Further Reading

Bickham, S. R., J. D. Kress, L. A. Collins, and R. Stumpf. 1999. *Ab Initio* Molecular Dynamics Studies of off-Center Displacements in CuCl. *Phys. Rev. Lett.* **83** (3): 568.

Collins, L. A., and A. L. Merts. 1985. Electronic Structure of Clusters of Atoms in a Dense Plasma. In *Proceedings of the 2nd International Conference on Radiative Properties of Hot Dense Matter, Sarasota, Florida, Oct. 31–Nov. 4, 1983*. Edited by J. Davis, C. Hooper, R. Lee, and A. Merts, 385. Singapore: World Scientific.

Desjarlais, M. P., J. D. Kress, and L. A. Collins. 2002. Electrical Conductivity for Warm, Dense Aluminum Plasmas and Liquids. *Phys. Rev. E* **66** (2): 025401 (R).

Kress, J. D., I. Kwon, and L. A. Collins. 1995. Simulation of Impurity Line Shapes in a Hot, Dense Plasma. *J. Quant. Spectros. Radiat. Transf.* **54** (1–2): 237.

Kress, J. D., S. R. Bickham, L. A. Collins, and B. L. Holian. 1999. Tight-Binding Molecular Dynamics of Shock Waves in Methane. *Phys. Rev. Lett.* **83** (19): 3896.

Kwon, I., L. A. Collins, J. D. Kress, N. Troullier, and D. L. Lynch. 1994. Molecular Dynamics Simulations of Hot, Dense Hydrogen. *Phys. Rev. E* **49**: R4771.

Lenosky, T. J., J. D. Kress, L. A. Collins. 1997. Molecular-Dynamics Modeling of the Hugoniot of Shock Liquid Deuterium. *Phys. Rev. B* **56** (9): 5164.

Mazevet, S., L. A. Collins, and J. D. Kress. 2002. Evolution of Ultracold Neutral Plasmas. *Phys. Rev. Lett.* **88** (5): 055001.

Mazevet, S., P. Blottiau, J. D. Kress, and L. A. Collins. 2004. Quantum Molecular Dynamics Simulations of Shocked Nitrogen Oxide. *Phys. Rev. B* **69**: 224207.

Mazevet, S., L. A. Collins, N. H. Magee, J. D. Kress, and J. J. Keady. 2003. Quantum Molecular Dynamics Calculations of Radiative Opacities. *Astron. Astrophys. Lett.* **405**: L5.

Mazevet, S., J. D. Johnson, J. D. Kress, L. A. Collins, and P. Blottiau. 2002. Density Functional Calculation of Multiple-Shock Hugoniots of Liquid Nitrogen. *Phys. Rev. B* **65**: 014204.

Militzer, B., D. M. Ceperley, J. D. Kress, J. D. Johnson, L. A. Collins, and S. Mazevet. 2001. Calculation of a Deuterium Double Shock Hugoniot from *Ab Initio* Simulations. *Phys. Rev. Lett.* **87** (27): 275502.

Saumon, D., and T. Guillot. 2004. Shock Compression of Deuterium and the Interiors of Jupiter and Saturn. *Astrophys. J.* **609** (2): 1170.

For further information, contact Lee A. Collins (505) 667-2100 (lac@lanl.gov).